Providence, RI
NOISE-CON 2016
2016 June 13–15

Experimental evaluation of equivalent-fluid models for melamine foam

Albert R. Allen [a)]
Noah H. Schiller [b)]
NASA Langley Research Center
Hampton, VA 23681, USA

ABSTRACT

Melamine foam is a soft porous material commonly used in noise control applications. Many models exist to represent porous materials at various levels of fidelity. This work focuses on rigid frame equivalent fluid models, which represent the foam as a fluid with a complex speed of sound and density. There are several empirical models available to determine these frequency dependent parameters based on an estimate of the material flow resistivity. Alternatively, these properties can be experimentally educed using an impedance tube setup. Since vibroacoustic models are generally sensitive to these properties, this paper assesses the accuracy of several empirical models relative to impedance tube measurements collected with melamine foam samples. Diffuse field sound absorption measurements collected using large test articles in a laboratory are also compared with absorption predictions determined using model-based and measured foam properties. Melamine foam slabs of various thicknesses are considered.

1 INTRODUCTION

Porous foams such as melamine have seen wide spread use in noise control applications. For example, in aerospace applications it is applied to the interior side of a fuselage or fairing to increase interior absorption and reduce exterior to interior noise transmission. One particular application of recent interest is the acoustic treatment of NASA's new Space Launch System (SLS).[1] The SLS will generate unprecedented thrust at liftoff. This will enable the vehicle to lift larger payloads than other rockets, however the extra thrust will also generate high acoustic environments. Excessive noise in the payload fairing could damage critical payload equipment. Consequently, a risk mitigation effort has been undertaken to develop new noise treatment strategies, such as hybrid systems involving structurally integrated resonant absorbers targeting low frequencies, along with broadband performing melamine foam slabs. The development of this type of hybrid noise treatment requires accurate models of both acoustic resonators and foam. While models of the resonant absorbers have been the focus of previous work[2–4], this paper focuses on identifying an acceptable model for the melamine foam.

There are numerous empirical and theoretical models available to model foam with different levels of fidelity[5]. This work focuses on relatively simple rigid-frame equivalent-fluid models,

[a)] email: albert.r.allen@nasa.gov
[b)] email: noah.h.schiller@nasa.gov

which represent the foam as a fluid with a complex-valued speed of sound and density. Accurate knowledge of equivalent-fluid properties is important when predicting system performance of the noise control package. There are several empirical models that provide estimates of these parameters based on measurements of the flow resistivity of the material. The primary goal of this work is to determine which of the empirical models, if any, accurately represent the melamine foam being considered for the SLS payload fairing application.

Foam material properties are ultimately used as inputs to other models, therefore an additional aspect of this work is to demonstrate and assess the accuracy of predicting acoustic metrics such as the diffuse field absorption coefficient using a wave-based technique. However, there is some ambiguity regarding the correct implementation of wave-based techniques when determining the absorption coefficient of finite test articles. As a result, a secondary goal of this work is to compare two finite corrections with recent ASTM C423-09a diffuse field absorption measurements involving finite foam slabs of various thicknesses recently collected by Hughes et al.[6].

This paper begins with a description of the melamine foam under consideration. Raylometer flow resistivity measurements are then discussed, and the procedure used to determine the bulk properties of the foam using a normal incidence plane wave tube is described. A comparison between some relevant empirical models and measurement educed properties is then provided. Finally, wave-based random incidence absorption coefficient predictions using two finite correction methods are compared with ASTM C423-09a absorption coefficient measurements of finite melamine foam slabs with various thicknesses and the resulting trends are discussed.

2 MELAMINE FOAM

The melamine foam used in this study was Soundcoat's Soundfoam MLULb foam, a lightweight (6.0 kg/m^3) foam formulated for reduced formaldehyde emissions. An image of the material is shown in Figure 1. Cuboid samples with 50.8 mm by 50.8 mm square cross sections and depths of 25.4 mm, 50.8 mm, 76.2 mm, 101.6 mm, and 203.2 mm were cut for testing in the NASA Langley Research Center (LaRC) Liner Technology Facility normal incidence tube and raylometer apparatuses for bulk property characterization[7]. Larger 2.743 m by 2.438 m MLULb slab test articles of various thicknesses were also subjected to diffuse field absorption testing at Riverbank Acoustical Laboratories during a previous study as described by Hughes, et al.[6].

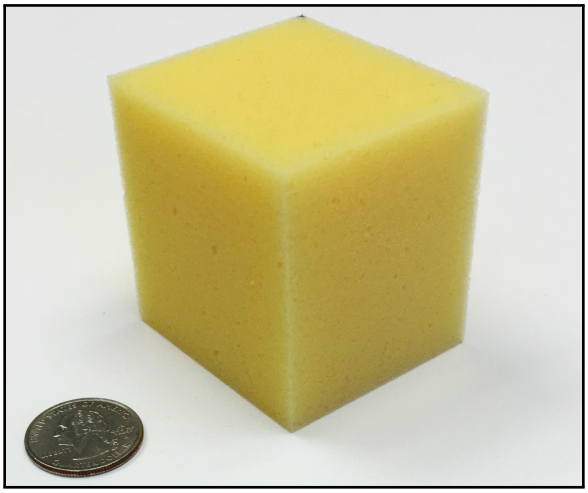

Figure 1: *Sample of MLULb foam.*

3 EMPIRICAL MODELS

There are numerous empirical and theoretical models that may be used to determine the complex-valued effective properties of a porous material. A recent evaluation of a number of these models has been provided by Oliva and Hongisto[8]. Most empirical models express the propagation constant Γ and characteristic impedance z_c in the material as complex exponential functions expressed as

$$z_c = z_0 \left(1 + C_1 X^{C_2} - jC_3 X^{C_4}\right) \tag{1}$$

and

$$\Gamma = k_0 \left(C_5 X^{C_6} + j\left(1 + C_7 X^{C_8}\right)\right), \tag{2}$$

where $z_0 = \rho_0 c_0$ is the specific impedance in air, $k_0 = 2\pi f/c_0$, $X = \rho_0 f/\sigma$, and σ is the specific flow resistivity in units of mks-rayl/m (Pa·s/m^2), and C_1–C_8 are empirically derived constants. These models are relatively easy to implement and only rely on the flow resistivity σ of the material, which is often provided by the manufacturer. Other more involved theoretical models require additional knowledge of less easily obtainable properties such as porosity, tortuosity, and viscous characteristic length. Consequently, only the single parameter empirical models following equations 1 and 2 will be considered here, and they will be further reduced to focus only on the Miki, Qunli, and Dunn & Davern models[9–11]. The Miki model was chosen because it is an improved version (reduced low frequency limitations) of the most well known Delaney & Bazley model. The models proposed by Qunli and Dunn & Davern were developed using polymer foam materials, so they were considered relatively more applicable for modeling MLULb. Coefficients for each of the considered models are provided in Table 1.

Table 1: Empirical model coefficients and coefficients determined from recent measurements.

Model	C_1	C_2	C_3	C_4	C_5	C_6	C_7	C_8
Miki	0.0700	-0.6320	0.1070	-0.6320	0.1600	-0.6180	0.1090	-0.6180
Qunli	0.2090	-0.5480	0.1050	-0.6070	0.1630	-0.5920	0.1880	-0.5540
Dunn & Davern	0.1140	-0.3690	0.0985	-0.7580	0.1680	-0.7150	0.1360	-0.4310
MLULb2016	0.0325	-0.8541	0.1804	-0.5630	0.2671	-0.5566	0.0401	-0.9238

4 EXPERIMENTAL DETERMINATION OF FOAM PROPERTIES

The flow resistivity of the foam was measured in the NASA LaRC raylometer. The raylometer is a test rig with a 50.8 mm square cross section that is used to evaluate the DC flow resistance of porous samples. Air is forced through the sample with a specified flow velocity v and the static pressure drop Δp across the material is measured. DC flow resistance is then estimated as $R_f = \Delta p/v$. Flow resistivity can then be calculated as $\sigma = R_f/d$, where d is the sample thickness. Typically, tests are repeated at progressively lower flow velocities until the DC flow resistivity converges, as shown in Figure 2. The flow resistivity of the MLULb samples was determined to be 9400 mks-rayl/m.

Various methods exist to measure the complex-valued bulk properties of porous media. Smith and Parrot[12] used a plane wave tube to compare the two-cavity and two-thickness methods over three decades ago. Both methods involved the measurement of two distinct, geometry-dependent surface impedances of a bulk absorber in a plane wave impedance tube. The two-thickness method was found to be more efficient. Consequently, this method was used to derive the characteristic impedance and propagation constant of MLULb based on normal incidence impedance measurements collected in

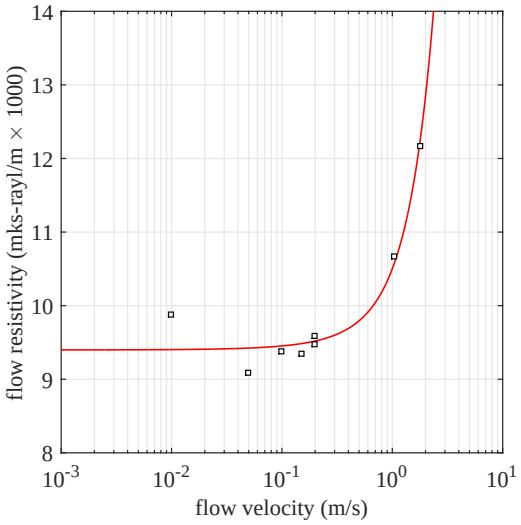

Figure 2: *Measured flow resistivity of a 25.4 mm cube MLULb sample (▫) and polynomial regression (—) vs. flow velocity.*

the normal incidence tube at NASA LaRC. The characteristic specific acoustic impedance z_c and propagation constant Γ in the foam are related to the the specific acoustic impedances at the surface of two foam samples of thicknesses d_1 and d_2 given by

$$z_{s1} = z_c \coth(\Gamma d_1) \qquad \text{and} \qquad z_{s2} = z_c \coth(\Gamma d_2) \tag{3}$$

If $d_2 = 2d_1$, the characteristic specific acoustic impedance and propagation constant can be expressed as

$$z_c = \sqrt{z_{s1}\left(2z_{s2} - z_{s1}\right)} \tag{4}$$

and

$$\Gamma = \frac{1}{2d_1}\ln\left(\frac{1+a}{1-a}\right), \tag{5}$$

where $a = \sqrt{\left(2z_{s2} - z_{s1}\right)/z_{s1}}$. The complex valued wavenumber, speed of sound, density, and bulk modulus in the sample are respectively given as

$$k = \frac{\Gamma}{j}, \qquad c = \frac{\omega}{k}, \qquad \rho = \frac{z_c}{c}, \qquad \text{and} \qquad K = z_c c, \tag{6}$$

where $\omega = 2\pi f$ and f is the frequency in Hz. The normal incidence surface impedance of a sample of thickness d can be rewritten in terms of the complex wavenumber k as

$$z_s = -jz_c \cot(kd), \tag{7}$$

and the normal incidence absorption coefficient of the sample in terms of the surface impedance can be written as

$$\alpha_{norm} = \frac{4\mathrm{Re}\left(\frac{z_s}{z_0}\right)}{\left|\frac{z_s}{z_0} + 1\right|^2}. \tag{8}$$

The complex bulk material properties were determined this way using samples with thicknesses of 25.4 mm, 50.8 mm, 76.2 mm, 101.6 mm, and 203.2 mm. Upon reviewing the results, it was

found that the longer two-thickness samples (101.6 mm and 203.2 mm) provided better results at low frequencies. Contrarily, the shorter samples (25.4 mm and 50.8 mm) provided results at higher frequencies that were less influenced by apparent frame dynamics. Results obtained from the two longest samples below 500 Hz and two shortest samples above 500 Hz were consequently combined for further analysis. Regressions were then performed separately on the real and imaginary parts of the characteristic impedance and propagation constant while adhering to the format of equations 1 and 2 resulting in coefficients C1-C8 as shown in Table 1 under *MLULb2016*.

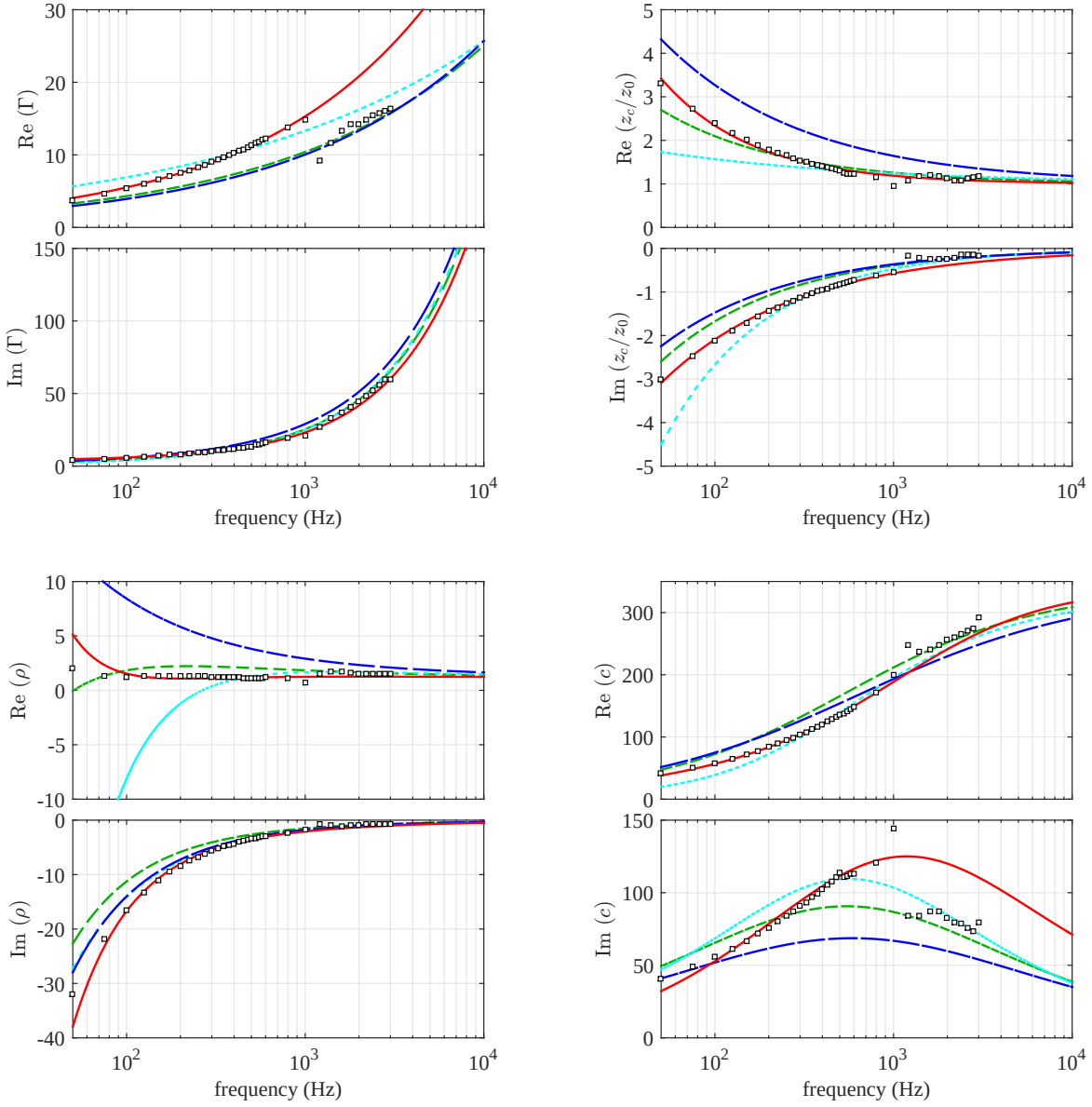

Figure 3: *Measured complex properties (▫) compared with models using coefficients from Miki (– –), Qunli (— —), Dunn & Davern (- -), and MLULb2016 (—).*

Comparison of the three considered empirical models, the MLULb2016 model, and the measured results are shown in Figure 3. Because the measured results were influenced by the geometry dependent frame dynamics at higher frequencies (particularly around 1 kHz), the measurement

regressions were heavily weighted toward the low frequencies. This is particularly evident when viewing $\mathrm{Re}\,(\Gamma)$ and $\mathrm{Re}\,(c)$. As a consequence of this, the MLULb2016 model is less accurate above 1 kHz. In the context of absorption coefficients, however, it will be shown that these differences are not very influential at higher frequencies. It should be noted that the measurement regressions leading to the MLULb2016 model were primarily used for further implementation in the absorption modeling procedures described herein. Creation of a statistically robust empirical model tailored toward melamine foams should be supported with further measurements.

5 NORMAL INCIDENCE ABSORPTION COEFFICIENT

An assessment of the aforementioned complex equivalent fluid properties was then made by comparing measured and modeled normal incidence absorption. Normal incidence absorption coefficient spectra determined using equation (8) and the empirical models defined in equations (1) and (2) and Table 1 are compared with measurement results in Figure 4. The measured results in this case were obtained from an independent 76.2 mm thick sample of MLULb that was not used when performing the measurement regression. As previously noticed when curve fitting the complex material properties, frame dynamic effects were found in the measured absorption coefficient near 1 kHz. Consequently, none of the equivalent fluid models are in particularly good agreement in this frequency region. The MLULb2016 model is in quite good agreement with the independent measurement below 1 kHz, which should be expected since all the normal incidence tube test samples were procured from the same foam slab and the curve fits were heavily weighted toward low frequencies. However, the three existing empirical models were considered sufficiently accurate for most practical engineering purposes. If any, Qunli's model was the least representative of MLULb out of the models considered. At frequencies above 1 kHz where the normal incidence absorption coefficient converges to 1, the Miki and Dunn & Davern models provided relatively better agreement with measurement.

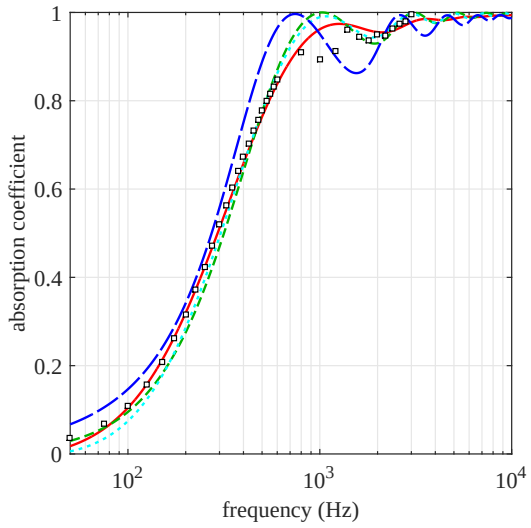

Figure 4: *Measured normal incidence absorption coefficient of a 76.2 mm thick MLULb sample (▫) compared with predictions determined using coefficients from Miki (– –), Qunli (— —), Dunn & Davern (- - -), and MLULb2016 (—) models.*

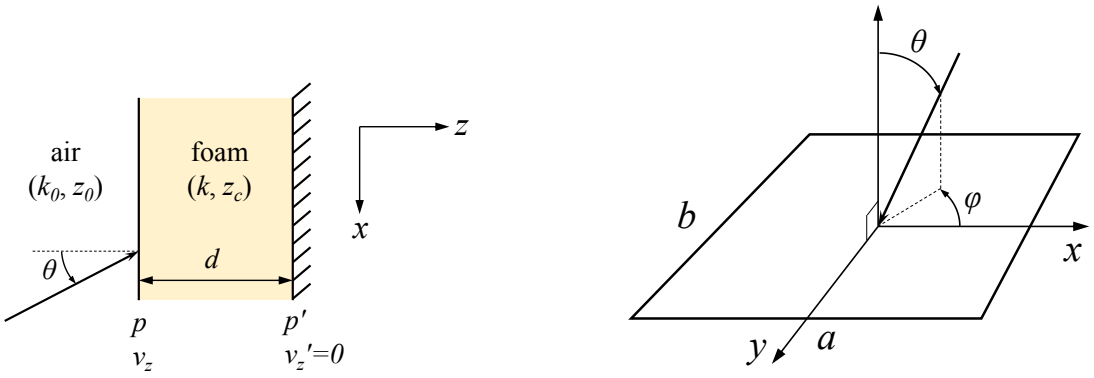

Figure 5: *Diagram of an incident wave impinging upon a single equivalent fluid foam layer (left) and a finite surface of dimensions $a \times b$ (right).*

6 RANDOM INCIDENCE ABSORPTION COEFFICIENT

For oblique incidence waves incident upon a foam slab of thickness d placed against a hard wall as shown in Figure 5, the surface impedance $z_s = p/v_z$ is now dependent on incidence angle such that

$$z_s = -j\frac{\omega\rho}{k_z}\cot(k_z d), \tag{9}$$

where $k_z = \sqrt{k^2 - k_0^2\sin(\theta)^2}$ is the z component of the wavenumber in the foam. The complex-valued wavenumber k and density ρ in the equivalent fluid foam are determined from equations 1, 2, and 6 as previously described.

Additionally, a finite foam layer is considered as a half-space baffled surface with specific surface impedance z_s and finite rectangular dimensions $a \times b$ as also shown in Figure 5. The oblique incidence absorption coefficient is the ratio of sound power absorbed by the surface to the sound power incident on the surface given as $\alpha(\theta, \phi) = W_{abs}/W_{inc}$. As detailed further in section 12.3 of Allard & Atalla[5], the incident and absorbed powers can be expressed as a function of the finite surface radiation impedance z_{rad} in order to account for the scattering and diffraction or "edge" effects often seen in absorption measurements and are given by

$$W_{inc,fin} = \frac{|\hat{p}_{inc}|^2 ab}{2z_0}\left(\frac{4\cos(\theta)}{\left|1 + \frac{z_{rad}}{z_0}\cos(\theta)\right|^2}\right) \tag{10}$$

and

$$W_{abs,fin} = \frac{|\hat{p}_{inc}|^2 ab}{2z_0}\left(\frac{4\mathrm{Re}\left(\frac{z_s}{z_0}\right)}{\left|\frac{z_s}{z_0} + \frac{z_{rad}}{z_0}\right|^2}\right), \tag{11}$$

where $|\hat{p}_{inc}|$ is the incident plane wave amplitude. Here, $W_{inc,fin}$ accounts for the geometric impedance seen by the incident wave and is equivalent to the power absorbed (transmitted) through an open window of similar geometry. To demonstrate this, the expression for $W_{inc,fin}$ can be found by replacing the surface impedance z_s with the "wall impedance" of an open window $z_0/\cos(\theta)$ in equation (11).

Brunskog[13] provided a means of calculating z_{rad} that is given by*

$$\frac{z_{rad}}{z_0} = \frac{jk_0}{2\pi ab}\int_0^a\int_0^b 4\cos(k_0\mu_x\kappa)\cos(k_0\mu_y\tau)\frac{\mathrm{e}^{-jk_0\sqrt{\kappa^2+\tau^2}}}{\sqrt{\kappa^2+\tau^2}}(a-\kappa)(b-\tau)\,\mathrm{d}\kappa\mathrm{d}\tau, \tag{12}$$

*Typographical errors pertaining to this equation were found in the reference.

where $\mu_x = \sin(\theta)\cos(\phi)$, $\mu_y = \sin(\theta)\sin(\phi)$, and $k_0 = 2\pi f/c_0$. Equation (12) was found to be amenable to numerical integration, but it was still computationally expensive to adequately resolve z_{rad} over θ, ϕ, and k_0. To speed up calculation times, the integrals in equation (12) were evaluated numerically for a range of k_0 and over incident and azimuthal angles comprising only one quarter of the hemisphere while making use of the quarter-symmetry of typical rectangular treatment surfaces. Results for a given rectangular aspect ratio were then saved to a database for quick recall and interpolation when calculating $W_{inc,fin}$ and $W_{abs,fin}$.

On the other hand, $z_{rad} = z_0/\cos(\theta)$ when considering a surface of infinite extent and the incident and absorbed powers simplify to

$$W_{inc,inf} = \frac{|\hat{p}_{inc}|^2 ab}{2z_0}\cos(\theta) \tag{13}$$

and

$$W_{abs,inf} = \frac{|\hat{p}_{inc}|^2 ab}{2z_0}\left(\frac{4\mathrm{Re}\left(\frac{z_s}{z_0}\right)}{\left|\frac{z_s}{z_0}+\frac{1}{\cos(\theta)}\right|^2}\right). \tag{14}$$

If only considering the normal incidence plane wave case, which is the situation in a plane wave tube, use of equations (13) and (14) leads to equation (8).

Because there is some ambiguity about how the finite size correction should be applied when determining the random incidence absorption coefficient of a finite absorber, i.e. to both absorbed and incident powers or to only absorbed power, three variations are considered here. By dividing out $|\hat{p}_{inc}|^2 ab/2z_0$ and integrating over incident and azimuthal angles, the random incidence absorption coefficients considered can be expressed as

$$\alpha_{inf} = \frac{\int_0^{2\pi}\int_0^{\pi/2} W_{abs,inf}\sin(\theta)\,\mathrm{d}\theta\mathrm{d}\phi}{\int_0^{2\pi}\int_0^{\pi/2} W_{inc,inf}\sin(\theta)\,\mathrm{d}\theta\mathrm{d}\phi}, \tag{15}$$

$$\alpha_{fin1} = \frac{\int_0^{2\pi}\int_0^{\pi/2} W_{abs,fin}\sin(\theta)\,\mathrm{d}\theta\mathrm{d}\phi}{\int_0^{2\pi}\int_0^{\pi/2} W_{inc,inf}\sin(\theta)\,\mathrm{d}\theta\mathrm{d}\phi}, \tag{16}$$

$$\alpha_{fin2} = \frac{\int_0^{2\pi}\int_0^{\pi/2} W_{abs,fin}\sin(\theta)\,\mathrm{d}\theta\mathrm{d}\phi}{\int_0^{2\pi}\int_0^{\pi/2} W_{inc,fin}\sin(\theta)\,\mathrm{d}\theta\mathrm{d}\phi}. \tag{17}$$

The measured Sabine absorption coefficients obtained from foam slabs of different thicknesses as described in Hughes et al.[6] are compared with modeled random incidence absorption coefficients using equations (15)–(17) in Figure 6. Only the MLULb2016 and Miki models were considered in this case. As the foam layer thickness increases, both the measurements and models show trends of increasing absorption at lower frequencies. This is a well known aspect that often precludes the use of compact (thin) foam noise treatments for low frequency noise reduction purposes. The effect of the finite geometry was also found to be significant in all cases. For example, use of the infinite surface absorption coefficient α_{inf} produced results that were considerably lower than measurement, especially at lower frequencies where the acoustic wavelength becomes large in relation to the size of the test article. Out of the three absorption coefficients considered, the doubly corrected α_{fin2} was found to be in better agreement when viewing frequencies near and below the thickness-dependent performance roll-off, e.g. near 250 Hz for the 101.6 mm case. However, this assessment was less obvious for the thickest slabs tested due to a possible room mode interaction at the 125 Hz 1/3 octave

band.[†] In general, the error attributed to choosing among the two empirical models considered was arguably small in relation to other biasing effects and measurement uncertainties.

Of particular interest is the bias in the modeled results at frequencies above the performance roll-off. All model variations converge to 1 at frequencies well above the performance roll-off, but the corresponding measured values exceed 1 and are typically 10% to 20% higher than the models for all but the three thinnest foam slabs. Two reasons for this phenomenon are proposed:

1. The radiation impedance z_{rad} used when accounting for the finite absorbing surface assumes a 2D finite surface while the actual test articles give rise to a 3D geometry when placed onto a flat hard surface. The 3D geometry may be promoting additional scattering and diffraction effects that are only partially accounted for in the 2D z_{rad}.

2. At high frequencies, the larger thicknesses provide additional vertical or edge-facing surface areas (in a geometric acoustic sense). As they become acoustically large at high frequencies, these additional absorbing surface areas may be biasing the measurements toward higher values relative to the modeling assumption that only considers the horizontal or top-facing surface area of the test article.

To shed light on this subject, further numerical simulations of the ASTM C423-09a procedure involving thick bulk reacting foam slabs is of interest.

7 CONCLUDING REMARKS

Complex bulk properties of MLULb, a melamine foam variety of recent interest, were measured using a raylometer and a normal incidence plane wave tube. The measurement educed equivalent fluid model (MLULb2016) was compared with three existing empirical models developed by Miki, Qunli, and Dunn & Davern. It was determined that use of any of the empirical models would suffice for practical engineering purposes, but selection of the MLULb2016 and Miki models may be preferred depending on the frequency range of interest. Diffuse field absorption coefficients (ASTM C423-09a) measured from finite MLULb slabs of various thicknesses were then compared with wave-based model predictions including two variants of the finite correction. Trends noticed in the results were discussed and further study regarding a discrepancy between measurement and model was motivated.

8 ACKNOWLEDGEMENTS

Experimental foam characterization was made possible through collaboration with Mike Jones, Carol Harrison, and Brian Howerton and utilization of the NASA LaRC Liner Technology Facility. Many thanks is also given to William Hughes, Anne McNelis, Chris Notolli, and Eric Wolfram for providing foam slab absorption measurement results taken at Riverbank Acoustical Laboratories.

[†]The limitations of room acoustic methods at low frequencies are widely known and well documented.

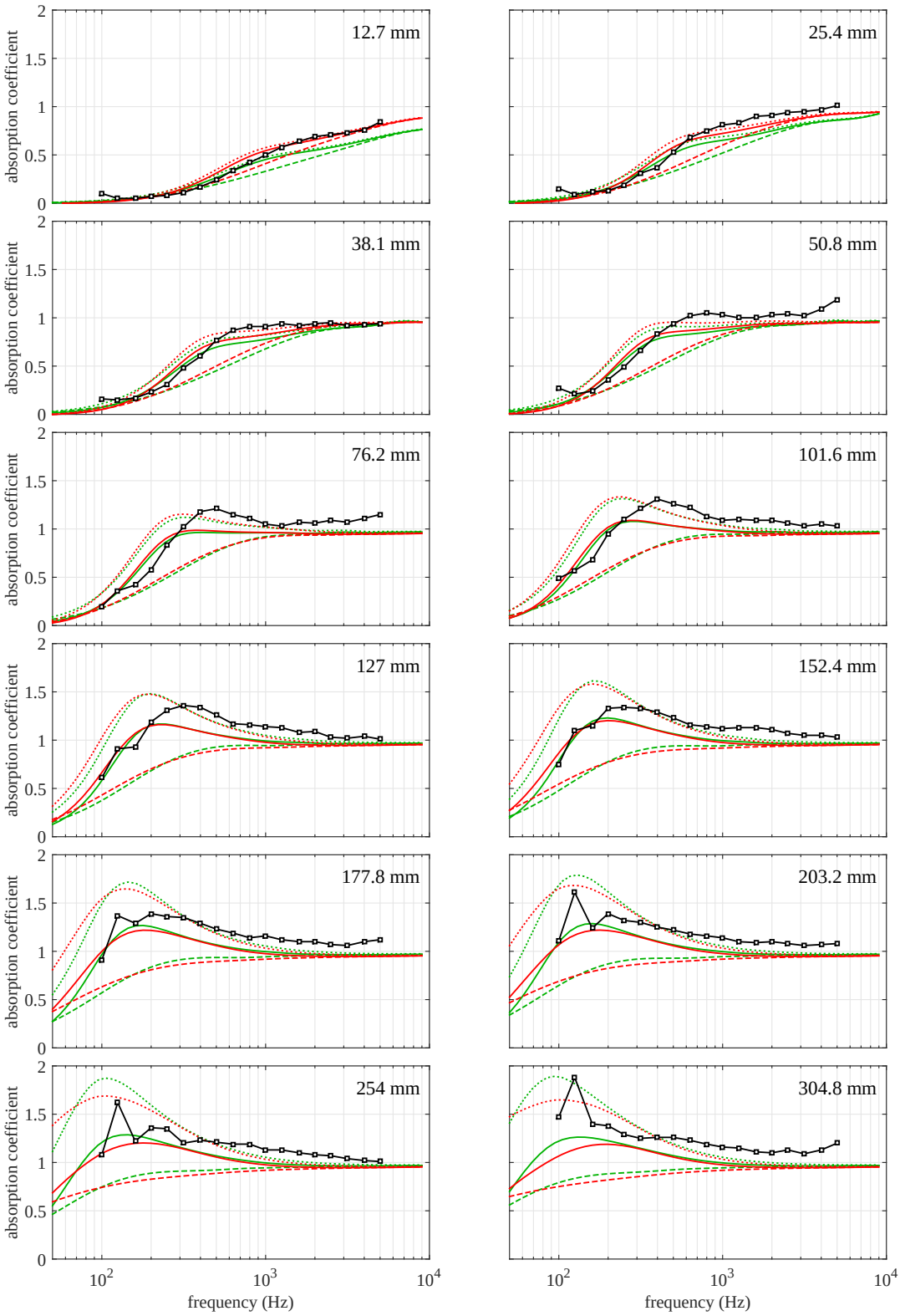

Figure 6: *Measured Sabine absorption coefficients (▫) of 2.743 m by 2.438 m MLULb foam slabs of various thicknesses compared with modelled random incidence absorption coefficients α_{inf} (– –), α_{fin1} (- - - -), and α_{fin2} (——) determined using material property coefficients from Miki (green) and MLULb2016 (red) models.*

9 REFERENCES

1. W. O. Hughes, A. M. McNelis, and M. E. McNelis, "Acoustic test characterization of melamine foam for usage in nasa's payload fairing acoustic attenuation systems," Tech. Rep. TM 2014-218127, NASA Glenn Research Center, 2014.
2. N. H. Schiller, A. R. Allen, B. F. Zalewski, and B. S. Beck, "Sound transmission loss through a corrugated-core sandwich panel with integrated acoustic resonators," in *Proceedings of the ASME 2014 International Mechanical Engineering Congress & Exposition*, (Montreal, Quebec, Canada), Nov. 2014.
3. A. R. Allen, N. H. Schiller, B. F. Zalewski, and B. Rosenthal, "Transmission loss and absorption of corrugated core sandwich panels with embedded resonators," in *Proceedings of NoiseCon 2014*, (Ft. Lauderdale, FL), Sept. 2014.
4. N. H. Schiller, A. R. Allen, J. W. Herlan, and B. N. Rosenthal, "Experimental evaluation of tuned chamber core panels for payload fairing noise control," in *Proceedings of the 29th Aerospace Testing Seminar*, (Los Angeles, California), Oct. 2015.
5. J. F. Allard and N. Atalla, *Propagation of sound in porous media*. Wiley, 2 ed., 2009.
6. W. O. Hughes, A. M. McNelis, C. Nottoli, and E. Wolfram, "Examination of the measurement of absorption using the reverberant room method for highly absorptive acoustic foam," in *Proceedings of the 29th Aerospace Testing Seminar*, (Los Angeles, California), Oct. 2015.
7. M. G. Jones and W. R. Watson, "On the use of experimental methods to improve confidence in educed impedance," in *Proceedings of the 17th AIAA/CEAS Aeroacoustics Conference*, (Portalnd, Oregon), June 2011.
8. D. Oliva and V. Hongisto, "Sound absorption of porous materials – accuracy of prediction methods," *Appl. Acoust.*, vol. 74, pp. 1473–1479, 2013.
9. Y. Miki, "Acoustical properties of porous materials – modifications of Delany–Bazley models," *J. Acoust. Soc. Jpn.*, vol. 11, pp. 19–24, 1990.
10. W. Qunli, "Empirical relations between acoustical properties and flow resistivity of porous plastic open–cell foam," *Appl. Acoust.*, vol. 25, pp. 141–148, 1988.
11. I. P. Dunn and W. A. Davern, "Calculation of acoustic impedance of multi–layer absorbers," *Appl. Acoust.*, vol. 19, pp. 321–334, 1986.
12. C. D. Smith and T. L. Parrott, "Comparison of three methods for measuring acoustic properties of bulk materials," *J. Acoust. Soc. Am.*, vol. 74, pp. 1577–1582, Nov. 1983.
13. J. Brunskog, "The forced sound transmission of finite single leaf walls using a variational technique," *J. Acoust. Soc. Am.*, vol. 132, pp. 1482–1493, Sept. 2012.